BIOCHEMISTRY
including biophysical chemistry & molecular biology

Accelerated Publication

pubs.acs.org/biochemistry

Spectroscopic Evidence of the Role of an Axial Ligand Histidinate in the Mechanism of Adrenal Cytochrome b_{561}

Giordano F. Z. da Silva, Vladimir P. Shinkarev, Yury A. Kamensky,* and Graham Palmer*

Department of Biochemistry and Cell Biology, Rice University, Houston, Texas 77251, United States

ABSTRACT: Adrenal cytochrome b_{561} (AdCytb) is the prototype of a widespread protein family that specializes in delivering electrons donated by ascorbic acid for different processes in eukaryotic cells. AdCytb transports redox equivalents from cytoplasmic ascorbate across the membranes of chromaffin granules to support norepinephrine synthesis within their matrix. The interaction of AdCytb with ascorbate is central to a proposed mechanism of AdCytb's function, and a histidine in the active site of AdCytb was suggested to bind cytoplasmic ascorbate and serve as the acceptor of the proton released during ascorbate oxidation. AdCytb contains high- and low-potential hemes but their orientation relative to the matrix and cytoplasmic interfaces of chromaffin granule membrane is disputed. Using a combination of three spectroscopic methods (UV−vis absorption, near-infrared magnetic circular dichroism, and electron paramagnetic resonance), we find that a histidine residue that serves as an axial ligand to the high-potential heme undergoes deprotonation with a pK of ∼8.0 and is thus a good candidate for interaction with cytoplasmic ascorbate. The low-potential heme of AdCytb is found to have a pK of ∼10.5, making it an unlikely candidate for accepting a proton at physiological pH. UV−vis spectroscopy reveals an additional proton acceptor group in AdCytb with a pK of ∼6.5 that is not observed by the other two techniques; whether it plays a role in the mechanism of AdCytb is unknown. We incorporate these results into an updated mechanism of AdCytb reduction predicated on the high-potential heme's localization on the cytoplasmic interface of the chromaffin granule membrane.

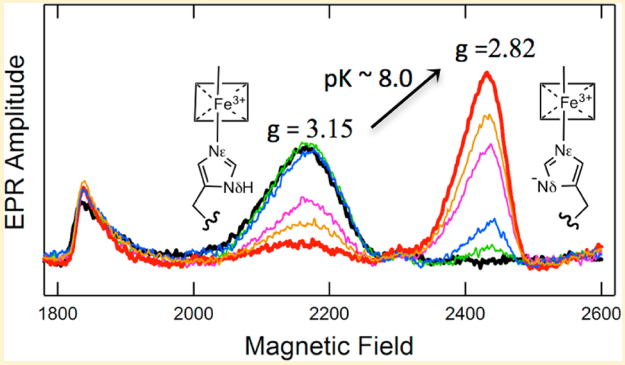

The cytochromes b_{561} are membranous electron-transfer proteins that appear to have evolved for transporting reducing equivalents donated by ascorbic acid across biological membranes.[10] The prototype of an extended protein family,[11] adrenal cytochrome b_{561} (AdCytb), shuttles electrons provided by cytosolic ascorbic acid of chromaffin cells to support norepinephrine synthesis in the matrix of chromaffin granules present in the medulla of adrenal glands.[5,12] AdCytb homologues in humans are important in a variety of different physiological situations: from cancer suppression in lungs[13] (101F6 gene product or TScytb) to maintenance of redox homeostasis in blood[14] (Dcytb in the membranes of erythrocytes) to transport of dietary iron in the duodenum[15] (Dcytb in the membrane of duodenal enterocytes). The members of this family are highly hydrophobic proteins with molecular masses typically around 30 kDa; they contain six transmembrane helices, four of which bind the two heme prosthetic groups by providing two pairs of histidines as axial ligands to the heme iron (Figure 1B). The midpoint redox potentials (E_m) of both hemes are moderately high (60 and 170 mV for AdCytb[6,7]). The heme centers of cytochromes b_{561} display two distinct low-spin EPR signals: in the case of AdCytb, the high-potential heme has a g_z of 3.12−3.16, while the low-potential heme belongs to the HALS class[a] and has a g_z of 3.69−3.72.[16−19]

Among the six members of the family present in humans, only AdCytb has been studied in detail from a physicochemical standpoint. It serves as a shuttle between the pools of cytoplasmic and granular ascorbate in chromaffin cells. Thus, peculiarly, AdCytb has the ascorbate/monodehydroascorbate redox couple serving as its reductant in the cytoplasm but as its oxidant in the matrix of chromaffin granules[20] (Figure 1A).

The two hemes of AdCytb are located on the opposite sides of the chromaffin granule membrane and thus are exposed to two very different environments: that of the cytoplasm (pH 7.2[21]) and that of the matrix (pH 5.5[20]). The disposition of high- and low-potential hemes of AdCytb within that model remains in dispute. According to Tsubaki et al.,[7,22−24] the high-potential heme (g_z = 3.1) is located on the matrix side of the membrane while the low-potential heme with a g_z of 3.7 is exposed to the cytoplasm; Kamensky et al.[19] and Liu et al.[25,26] have argued in favor of the opposite heme topology. The disposition of hemes in several plant homologues of AdCytb led to a similar controversy (Cenacchi et al.[27] and Nakanishi et al.[28] vs Desmet et al.[29]).

The first general mechanism of oxidation of ascorbate by AdCytb was proposed by Njus, Kelley, and co-workers.[5,8,30] Its

Received: August 20, 2012
Revised: October 10, 2012
Published: October 22, 2012

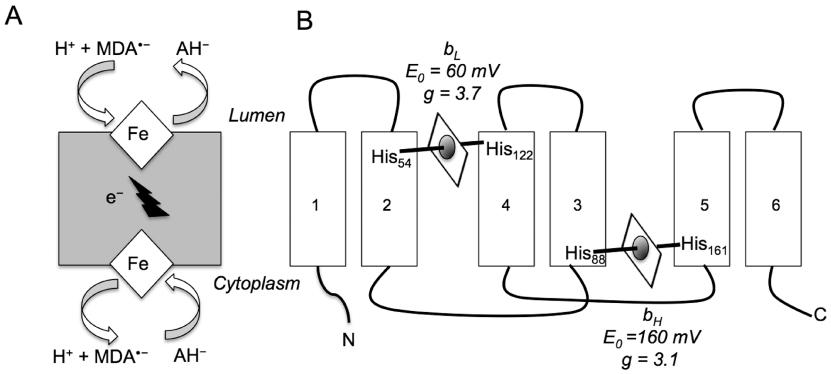

Figure 1. Electron transport via AdCytb (A) and the topological arrangement of AdCytb in the membrane of chromaffin granules (B). (A) According to the current paradigm, cytoplasmic ascorbate (AH^-) is oxidized by AdCytb to monodehydroascorbate ($MDA^{\bullet-}$). The resulting electrons are transferred to the lumen (matrix) of chromaffin granules to replenish ascorbate consumed in the process of norepinephrine synthesis by reducing intragranular $MDA^{\bullet-}$. (B) The transmembrane helices of AdCytb numbered 1−6 are connected by the extramembrane segments. Two hemes are bound to the apoprotein by histidine residues 122 and 54 and histidine residues 161 and 88. The cross-linked binding of hemes to the four central helices constitutes a "core domain" (note that the order of helices 3 and 4 is inverted for the sake of clarity). The location of the high-potential heme close to the cytoplasmic interface of AdCytb is based on previous mutagenic studies[19,25,26,29] and the hypothesis advanced in this article.

key element is the abstraction of an H atom from ascorbate in the process of a concerted H^+/e^- transfer, facilitated by an imidazole group of a histidine located somewhere on the cytoplasmic interface of AdCytb. The choice of histidine as the proton acceptor was guided by experiments in the groups of Njus and Tsubaki, in which the treatment of membranous AdCytb[5,8,31] and of purified protein[7,22,23] with the relatively specific histidine modifier, diethyl pyrocarbonate (DEPC), affected the level and the kinetics of reduction of the AdCytb with ascorbate, as well as its redox potential. As DEPC binds preferentially to unprotonated histidine, these experiments suggested that one of the histidine residues on the extravesicular side is a potential proton acceptor. Furthermore, the thermodynamics of ascorbate oxidation[5] and the molecular modeling of the interaction of ascorbate with the imidazole group of histidine[8] prompted Njus et al. to favor coupled H^+/e^- versus pure electron transfer.

Tsubaki and his colleagues[24] modified the Njus−Kelley mechanism by assigning the role of the proton acceptor specifically to an axial ligand of the heme located at the cytoplasmic interface of the chromaffin granule membrane (either His161 or His88) (Figure 1B). This modification of the original AdCytb mechanism was recently supported in model studies in which the reduction of an unprotonated porphyrin imidazole by an ascorbate derivative occurred more than 10 times faster than the reduction of a protonated compound.[32]

The imidazole ring of histidine contains two nitrogen atoms at positions ε_2 and δ_1 (Figure 2), of which $N\varepsilon_2$ provides coordination to heme iron in the majority of histidine-ligated hemeproteins.[b] When coordinated to iron, $N\varepsilon_2$ cannot bind a proton but is readily protonated (pK = 6−7; $HisH^+$) in histidine residues not bound to heme iron. On the other hand, $N\delta_1$ is adjacent to the β-C atom (Figure 2) and can exist in either the protonated (neutral histidine, HisH) or deprotonated form (histidinate anion, His^-), but its pK is very different depending on whether $N\varepsilon_2$ of the histidine is coordinated to heme iron. In solutions of free imidazole, $N\delta_1$ has a pK of 14.5.[33] Coordination of a histidine to heme iron[34] and its further stabilization with a hydrogen bond to a neighboring side group lower the pK of $N\delta_1$.[35]

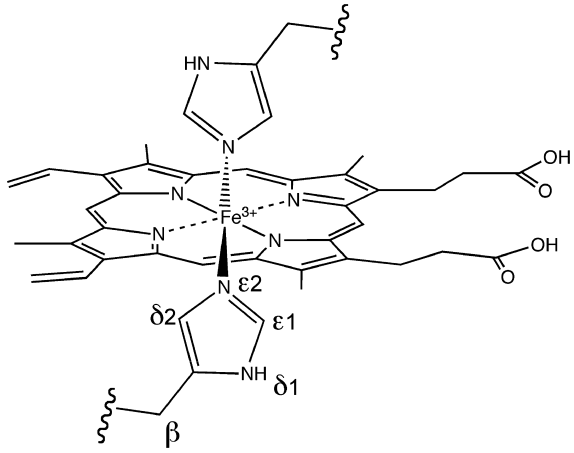

Figure 2. Structure of bis-histidine-coordinated heme (PPIX). The atom numbering is the same for both histidine residues.

In extreme cases, the pK can fall by as much as 7 units (a complex of leghemoglobin with imidazole[36]), but more typical values of $N\delta_1$ pK are in the range from 9.0 for cytochrome b_{562} from *Escherichia coli*[35] to 10.5 for an imidazole complex of metmyoglobin.[34]

To serve as an acceptor of protons from cytoplasmic ascorbate, the axial histidine to the heme present at the cytoplasmic interface of AdCytb should be at least partially deprotonated at physiological pH. The appearance of an EPR signal, traditionally associated with histidinate (the histidinate form, g_z around 2.8[37]), was noticed by Tsubaki et al. in a sample of AdCytb purified from chromaffin vesicles[18] but dismissed by the authors as an artifact of high pH.[18,38] The pH dependence of heme with a g_z of 3.70 has not been investigated.

To further explore the general mechanism of ascorbate oxidation by AdCytb, we subjected the cytochrome to pH titrations while monitoring possible changes with several spectroscopic techniques. The data reveal the presence of two pK values associated with the axial ligands; at least one of these axial ligands is a good candidate as a proton acceptor during ascorbate oxidation.

dx.doi.org/10.1021/bi301127k | *Biochemistry* 2012, 51, 8730−8742

EXPERIMENTAL PROCEDURES

Materials. Hemin, δ-aminolevulinic acid, MES, MOPS, TAPS, CAPS, lysozyme, benzonase nuclease, imidazole, ascorbic acid, sodium deuteroxide (NaOD), deuterium chloride (DCl), ampicillin, and chloramphenicol were from Sigma (St. Louis, MO). Protease inhibitor cocktail Set I (without EDTA) and IPTG were from Calbiochem (San Diego, CA). D_2O was from Cambridge Isotope Laboratories (Andover, MA). Luria-Bertani broth, Luria Bertani agar, and Terrific Broth (modified) were from Research Products International Corp. (Mt. Prospect, IL). The universal pH indicator was from RICCA Chemical Corp. (Arlington, TX). *n*-Dodecyl β-D-maltoside was from Affymetrix (Maumee, OH). HisPur cobalt resin was from Fisher (Swanee, GA). 10-DG desalting columns were from Bio-Rad. *E. coli* strain BL21Star(DE3) was purchased from Invitrogen (Carlsbad, CA) and modified with the chaperone plasmid pT-groE [generously provided by L.-H. Wang (University of Texas Health Science Center at Houston, Houston, TX)] to generate the expression strain used throughout the experiments. Plasmid vector pET43.1a was from Novagen (Madison, WI).

Recombinant AdCytb Expression. Recombinant bovine AdCytb was expressed in *E. coli* according to published methods[39] with modifications to fit this study. Plasmid vector pET43.1a containing the cDNA encoding AdCytb was transformed into the BL21Star/pT-groE *E. coli* strain, plated, and selected on LB-agar-amp plates containing 200 μg/mL ampicillin and propagated in LB medium containing 200 μg/mL ampicillin and 34 μg/mL chloramphenicol at 37 °C while being shaken at 200 rpm overnight as starter cultures. Terrific Broth medium (500 mL) containing 200 μg/mL ampicillin was inoculated with 5 mL of the overnight starter cultures and shaken at 37 °C and 200 rpm until the OD_{600} reached ~0.6. The expression cultures were then immediately placed in an ice bath for 20 min, with subsequent addition of 5 μM heme, 300 μM ALA, and 1.0 mM IPTG. Cultures were shaken at 16 °C and 200 rpm for 48 h, harvested by centrifugation at 4500 rpm, and either stored at −78 °C or immediately used for purification.

"Buffer A" for pH-Dependent Studies. "Buffer A" contained equimolar amounts of Good buffers (75.0 mM MES, MOPS, TAPS, and CAPS),[40] with addition of DM and/or glycerol, as specified in the text, according to experimental requirements.

Recombinant AdCytb Purification. Recombinant AdCytb was purified according to previously established protocols[39] with modifications to fit this study. Cells from 12 L of culture were resuspended in 400 mL of "Buffer A" containing 5% (v/v) glycerol (pH 7.2). Egg lysozyme (0.6 g in 12 mL of "Buffer A") was added to the slurry and the mixture stirred at 4 °C for 2 h followed by sonication (100 mL portions, 12 min; 5 s intervals, 60% duty cycle). Lysed cells were centrifuged at 100000*g* and 4 °C for 1 h. The pellet (membrane fraction containing recombinant AdCytb) was resuspended with 200 mL of "Buffer A" (pH 7.2) containing 5% (v/v) glycerol and 2% (w/v) DM, 5 mM $MgCl_2$, 10 μL of benzonase nuclease, and 100 μL of Protease Inhibitor Cocktail Set I and stirred at 4 °C overnight. Unextracted material was pelleted by centrifugation at 100000*g* and 4 °C for 1 h, and the pH of the supernatant was adjusted to 7.3−7.5. A 5 mL portion of HisPur resin was washed with 10 bed volumes of deionized water and 10 bed volumes of "Buffer A" (pH 7.2) containing 0.3 M NaCl, 20% glycerol, and 0.1% DM. The resin was added to the supernatant and then gently stirred at 4 °C for 2 h. The suspension was then added to a column, and the flow-through was collected. One wash was performed at room temperature with 10 bed volumes of "Buffer A" (pH 7.2) containing 0.3 M NaCl, 20% glycerol, and 0.1% DM. A second wash was performed using 10 volumes of "Buffer A" (pH 7.2) containing 20% glycerol, 20 mM imidazole, and 0.1% DM. The His-tagged recombinant protein was eluted from the affinity resin by 10 bed volumes of "Buffer A" (pH 7.2) containing 20% glycerol, 0.1% DM, and 200 mM imidazole. Eluent containing recombinant AdCytb was pooled on the basis of the A_{415}/A_{280} ratio (>3), concentrated to 1 mL using a Centriprep device (Millipore Corp.) with a molecular mass cutoff of 30 or 100 kDa, and then chromatographed on a 10-DG column, equilibrated with "Buffer A" (pH 7.2) containing 20% glycerol and 0.1% DM to remove imidazole.

Preparation of Samples for nIR-MCD Measurements. Samples were prepared by purification steps described above but using buffers prepared with D_2O, without glycerol, and the pD was adjusted using DCl and NaOD.

Electronic Absorption Spectroscopy. The electronic absorption spectra were recorded using JASCO V-560 nm and Cary-100 spectrophotometers with 0.05 nm increments, a 2 nm bandwidth, and a scanning speed of 30 nm/min. A 3.0 mL sample of AdCytb was adjusted to the appropriate pH values with small additions of HCl and NaOH in a quartz cuvette with a 10 mm path and allowed to equilibrate for 5 min, and the final pH value was directly measured in the cuvette. Spectra were collected between 350 and 700 nm. "Buffer A" containing 0.1% DM and 20% glycerol was used.

Analysis of Absorbance Changes. Absorbance changes were analyzed using Matlab (version 6.1, The Mathworks, Inc.) and Origin (version 6.1, OriginLab Corp.). The pretreatment of experimental data sets included FFT 15-point smoothing, as implemented in Origin; the absorption and wavelength values were compressed to reduce the number of points (from 5401 in each experimental spectrum to 270) followed by a three-point moving average of the compressed data with respect to the pH changes. Each operational step described above was carefully monitored to ensure that no particular procedure had modified the spectra or their resolution. The p*K* values and the amplitudes of each species were determined individually for each wavelength, using the function 'lsqcurvefit' in the Matlab Optimization Toolbox, or by using a nonlinear curve fitting module in Origin.

nIR−Magnetic Circular Dichroism. The MCD spectra were acquired with a JASCO J-730-NIR CD/MCD spectrometer at room temperature. A 150 W tungsten−halogen lamp and a liquid nitrogen-cooled high-sensitivity InSb detector equipped with a 1.4 T electromagnet were used. CD wavelength and sensitivity were calibrated with a 1:1 mixture of 0.24 M $NiSO_4$ and 0.36 M K^+,Na^+-D-tartrate. Spectra were collected between 700 and 1850 nm with 1 nm step resolution, with a scanning speed of 500 nm/min, at a bandwidth of 10 nm, with a time constant of 1 s. The MCD spectra calculated from H^+ (CD + MCD) and H^- (CD − MCD) were adjusted for the molar delta absorption coefficient, ΔA $(M\ cm\ T)^{-1}$.

A pD-dependent nIR-MCD study was performed using a 1.2 mL sample of AdCytb with a heme concentration of 200 μM. AdCytb was placed in a quartz cuvette with a 10 mm path, and the pD was judiciously adjusted with small additions of dilute solutions of DCl and NaOD (in D_2O). The sample was allowed

to equilibrate for 5 min, and the final pH was assessed directly in the cuvette, using a pH meter. The pD was calculated by using the approximation of pD = pH meter reading + 0.4. "Buffer A" prepared with D_2O containing 0.1% DM was used.

EPR Spectroscopy. The EPR spectra were recorded at 8 K with a Bruker EMX300 spectrometer equipped with a liquid helium cryostat. A total of seven samples of 400 μL of Adcytb (106 μM heme) were prepared to the desired pH by additions of small amounts of HCl and NaOH solutions and allowed to equilibrate for 5 min. "Buffer A" containing 0.1% DM and 20% glycerol was used. The pH was measured directly in the samples with a pH meter prior to them being placed into an EPR tube and rapidly frozen (~1 s) by plunging into an ethanol/dry ice bath and then transferred to liquid nitrogen for storage. To verify whether the pH of the buffer shifts on freezing, the calibration was performed by adding a universal pH indicator to "Buffer A" containing 50% glycerol. Two identical sets of buffer samples at pH values between 5.0 and 10.0 in 0.5 pH unit increments were placed in EPR tubes. One set of the buffer samples was frozen in the mix of dry ice and ethanol (approximately −75 °C), while the other was left at room temperature. The colors of frozen and liquid duplicate samples were then compared by visual inspection.

RESULTS

pH Dependence of EPR Spectra of Ferric AdCytb. Between pH 5.5 and 7.0, ferric AdCytb displays two distinct low-spin EPR signals: a conventional low-spin signal with a g_z of 3.15 and a g_y of 2.23 and a HALS-type signal with a g_z of 3.72 (Figure 3b). These are familiar features for the high- and low-potential hemes of AdCytb, respectively, previously observed in its membranous[16,17] and purified[18,19] samples. The g = 4.3 signal represents non-heme iron; the g = 6 signal belongs to a small amount of high-spin heme. A small g = 2.02/1.99 signal is not related to the hemes of AdCytb and is currently of unknown origin (Figure 3a).

When the pH changes from 7.0 to 9.0, the amplitude of the g_z = 3.15 signal gradually decreases and a new g_z = 2.82, g_y = 2.23, g_x = 1.67 low-spin species appears in a reciprocal manner (Figure 3). Species with these EPR parameters were previously identified as hemeproteins with one of the axial ligand histidines deprotonated at Nδ_1.[35,37,41−44] The amplitude of the low-potential heme (g_z = 3.72) is not affected by pH increases until the pH reaches 9.5 (Figure 3b), and thus, the emerging signal of His^--AdCytb at g_z = 2.82 is solely the product of deprotonation of the high-potential heme with a g_z of 3.15. The amplitude of the g_z = 3.15 signal at pH 9.0 is approximately 10% of its original amplitude at pH 7.0 (Figure 3b), which implies 90% conversion into the deprotonated species at pH 9.0. The Henderson−Hasselbalch equation for a single component with a pK of 8.0 approximates well the changes in the amplitude of the g_z = 2.82 signal, as shown in the inset of Figure 3b.

From neutral pH and until pH 9.0, the low-potential HALS heme does not undergo any changes. Between pH 9.0 and 9.5, the amplitude of the g_z = 3.72 signal decreases for the first time and is accompanied by a further increase in the magnitude of the g_z = 2.82 signal (Figure 3b). We interpret this as signifying the deprotonation of a low-potential heme in AdCytb; this has not been reported previously. Above pH 9.5, the behavior of HALS becomes complex (Figures 3b and 4). A part of the heme undergoes further deprotonation as reflected in the growth of the g_z = 2.82 signal until the pH reaches 12. A second

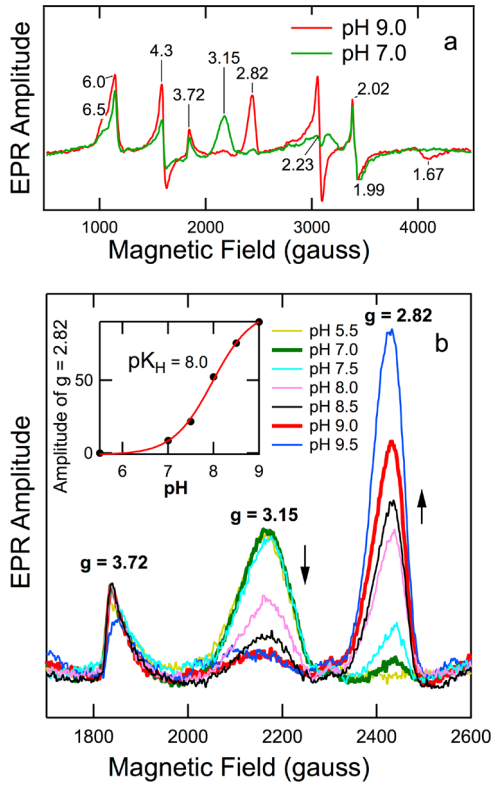

Figure 3. EPR spectra of AdCytb at different pH values. Spectra were recorded at 8 K with a microwave power of 4 mW. Other spectrometer settings were as follows: microwave frequency, 9.58 GHz; modulation frequency, 100 kHz; modulation amplitude, 10.9 G. Each sample was prepared from the same stock of AdCytb in "Buffer A" containing 0.1% DM and 20% glycerol. The final heme concentration of each sample was 106 μM. The pH was adjusted and measured in each sample prior to it being frozen. (a) Wide scan EPR spectra of AdCytb at pH 7.0 and 9.0. The g_z = 3.15, g_y = 2.23 signal is converted into the g_z = 2.82, g_y = 2.23, g_x = 1.67 signal as a function of pH. (b) Low-spin heme region of the EPR spectra of AdCytb at different pH values. With a pH increase from 5.5 to 9.0, the g_z = 3.15 signal amplitude decreases, while the g_z = 2.82 signal amplitude grows in a reciprocal manner. A further change in pH from 9.0 to 9.5 causes the decrease in amplitude of the g_z = 3.72 signal, accompanied by the additional growth of the magnitude of the g_z = 2.82 signal. In the inset, the amplitude of the g_z = 2.82 signal is plotted as a function of pH and fit using the Henderson−Hasselbalch equation, yielding a single pK of 8.0.

part of the g_z = 3.72 heme is converted into the high-spin species that is visible at g = 6.0/6.5. This high-spin signal became progressively heterogeneous with increasing pH but remains a minor contribution relative to the low-spin species (Figure 4). Finally, some part of the g_z = 3.72 heme apparently loses its iron above pH 11, so that the non-heme iron g = 4.3 signal dominates the EPR spectrum at pH 12 (shown partially in Figure 4). The shape of the HALS signal undergoes characteristic changes between pH 11 and 12 with the appearance of a broad, nondescript peak underneath the g_z = 3.72 resonance that is reminiscent of the signals of AdCytb axial ligand mutants.[19] As a number of processes are occurring simultaneously, the deprotonation of the HALS heme cannot be uniquely described by a single Henderson−Hasselbalch equation as was done for the heme with a g_z of 2.82 (Figure 3a, inset). Nevertheless, an estimate of the pK characterizing the process of deprotonation of the HALS heme can be obtained if we assume that it proceeds like the deprotonation of the g_z =

dx.doi.org/10.1021/bi301127k | Biochemistry 2012, 51, 8730−8742

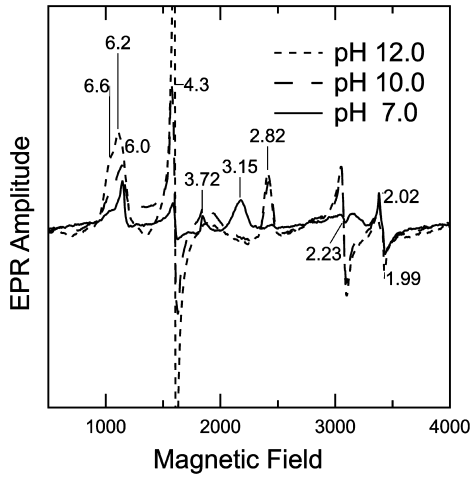

Figure 4. EPR spectra of AdCytb at higher pH values. Wide scan spectra of AdCytb at pH 10.0 and 12.0 in comparison with that at pH 7.0. Experimental conditions and spectrometer settings are the same as those in Figure 3.

3.15 species and that the process starts between pH 9.0 and 9.5 and is complete by pH 12.0, predicting a p*K* of approximately 10.5.

The possibility of a shift in the pH of the buffer solution during freezing was a concern.[45−47] Even though only a single buffer is needed to maintain the pH near its p*K*, we employed an equimolar mixture of four buffers initially introduced by Good et al.[40] to prevent potential unspecific effects at one pH but not at others (see Experimental Procedures). Good buffers are known for their relatively small temperature dependence on freezing.[45] The pH values of the frozen samples were verified by calibrating "Buffer A" using a universal pH indicator (see Experimental Procedures), as recommended by Williams-Smith et al.[47] We found that above pH 7.0 freezing caused pH increases of 0.25−0.5 unit; thus, the p*K* value for the histidine−histidinate transition of the high-potential heme derived from our EPR experiment (Figure 3b, inset) should be placed in the interval of pH 8.0−8.5.

Near-Infrared Spectra of Magnetic Circular Dichroism of Oxidized AdCytb. The magnetic circular dichroism spectra in the near-infrared region (700−1850 nm) (nIR-MCD) of purified ferric AdCytb were measured between pD 6.6 and 11.8 at room temperature in the mixture of Good buffers prepared in D_2O (Figure 5). At the lower pD values, we observed a pattern of two bands for the AdCytb hemes with λ_{CT} values typical for bis-imidazole ligation for low-spin hemes.[48] Both absorptions are porphyrin-to-Fe charge-transfer bands; the intense feature, caused by the $a_{1u} \rightarrow d\pi$ transition, has a maximum at 1610 nm, while the weaker feature (due to the $a_{2u} \rightarrow d\pi$ transition) is located near 1350 nm. A minor species with a maximum at ∼1050 nm is possibly a vibrational transition associated with the main bands, although the existence of a minor fraction of heme with histidine/hydroxide ligation cannot be excluded.[34]

Unlike the case of the two hemes of mitochondrial cytochrome *b*, which exhibit two distinct $a_{1u} \rightarrow d\pi$ transitions at 1590 and 1660 nm,[49] the charge-transfer bands of the two hemes of AdCytb fortuitously have similar MCD characteristics, and given the broadness of the bands, the individual spectra are practically indistinguishable. Only at the highest pD values, when one heme is fully deprotonated and shifts its position

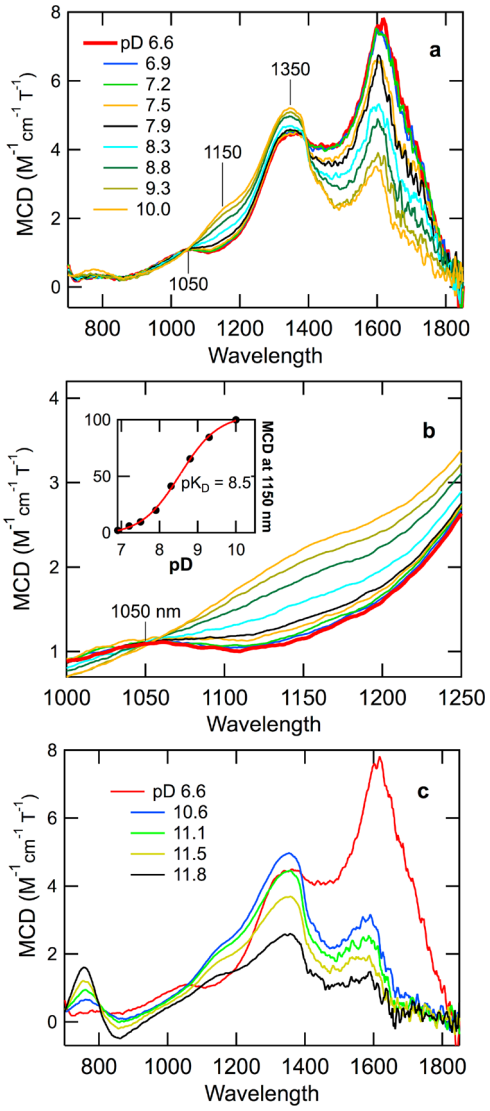

Figure 5. nIR-MCD spectra of ferric AdCytb at different pD values. A 200 μM solution (heme concentration) of AdCytb was prepared in "Buffer A" (made in D_2O) containing 0.1% DM and 20% glycerol; the pD (pH meter reading + 0.4) was initially adjusted to 6.6 using DCl and increased stepwise in the course of the experiment with controlled additions of NaOD. The spectra were recorded at room temperature using a JASCO J-730-NIR CD/MCD spectrometer equipped with a 1.4 T electromagnet in a 10 mm cuvette. The spectrometer settings were as follows: scanning speed, 500 nm/min; bandwidth, 10 nm; time constant, 1 s. (a) Wide scan spectra of AdCytb at different pD values. (b) Expanded spectra showing an increase in the amplitude at 1150 nm, a wavelength diagnostic of histidinate formation. The inset shows the normalized change in amplitude at 1150 nm plotted as a function of pD and fit using the Henderson−Hasselbalch equation, yielding a single pK_D of 8.5 (p*K* = 8.1). (c) Wide scan spectra of AdCytb at the highest pD values.

(Figure 5c), can one assess the parameters of the MCD spectrum of the second heme individually; it has its maximum at ∼1590 nm (Figure 5c)

Increasing the pD above 7.0 induces the appearance of an additional low-spin species with an intense feature ($a_{1u} \rightarrow d\pi$) located at 1350 nm. The weaker feature ($a_{2u} \rightarrow d\pi$) of the new species is located at 1150 nm (Figure 5a). A pair of charge-transfer bands with maxima at 1350 and 1150 nm was previously attributed to histidine−histidinate axial liga-

dx.doi.org/10.1021/bi301127k | *Biochemistry* 2012, 51, 8730−8742

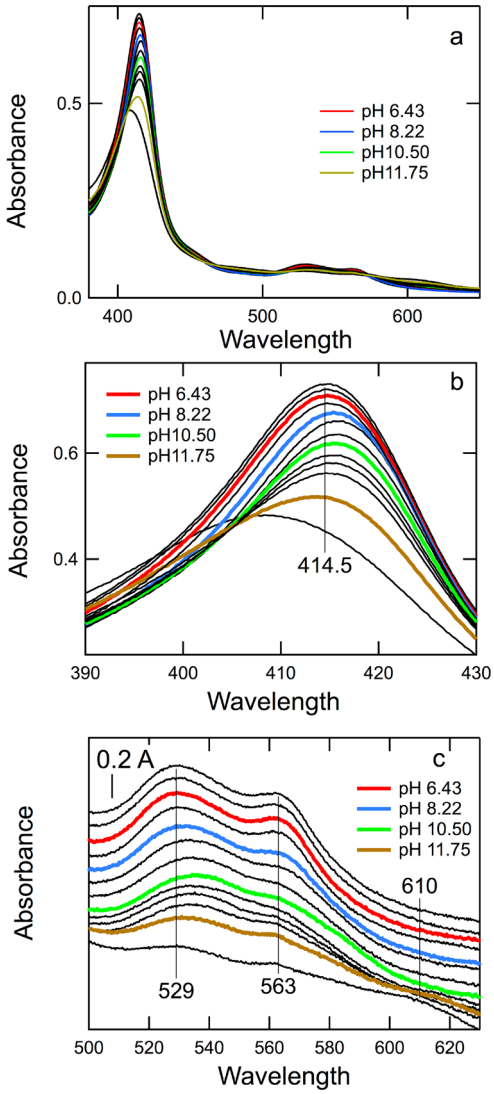

Figure 6. Absorption spectra of oxidized AdCytb at different pH values. Ferric AdCytb (5.9 μM) was studied in "Buffer A" in the presence of 20% glycerol. A total of 32 pH values were used in the experiment; selected spectra collected at pH 5.76, 5.92, 6.43, 7.16, 8.22, 9.19, 10.12, 10.50, 10.91, 11.13, 11.40, 11.75, and 12.05 are presented in panels a–c. The spectra were recorded using a Cary-100 spectrophotometer with 0.05 nm increments, a 2 nm bandwidth, and a scanning speed of 30 nm/min in a 10 mm cuvette. (a) Absorption spectra of oxidized AdCytb collected between 380 and 650 nm. (b) Expanded spectra in the Soret region. (c) Expanded spectra in the visible region. The spectra in panel c have been shifted vertically for the sake of clarity. The colored traces correspond to the pK of transitions between pH states A–E of AdCytb (Figure 7) calculated according to Scheme 1.

Scheme 1

$$A \xleftrightarrow{pK1} B \xleftrightarrow{pK2} C \xleftrightarrow{pK3} D \xleftrightarrow{pK4} E$$

tion.[34,36,50] At 1350 nm, the weak feature ($a_{2u} \rightarrow d\pi$) of the protonated heme and the intense feature ($a_{1u} \rightarrow d\pi$) of the deprotonated heme are fortuitously overlapping; consequently, to characterize the transformation of HisH to His^-, we utilized the latter's weaker band at 1150 nm (Figure 5b). The dependence of the amplitude of MCD absorption at 1150 nm in the pD interval between 6.6 and 10.0 is fit well with the Henderson–Hasselbalch equation with a pK in D_2O of 8.5 (Figure 5b, inset); this corresponds to a pK of 8.1 in H_2O.

When the pD is increased above 10, the signal of the high-spin heme[48] appears, centered at 800 nm (Figure 5c). It occurs simultaneously with the decrease in the amplitude of the signals at 1650, 1350, and 1150 nm (Figure 5c). An approximate estimate of the formation of the high-spin species of AdCytb yields a pK value in D_2O of 11.6 (not shown).

Absorption Spectra of Oxidized AdCytb at Different pH Values. The absorption spectra of oxidized AdCytb were recorded from 380 to 650 nm over the pH range from 5.76 to 12.05 in increments of approximately 0.2 pH unit (Figure 6), achieved by the addition of aliquots of NaOH. At acid and neutral pH, the spectra are typical for a low-spin cytochrome of b type with a Soret maximum at ~415 nm and α/β bands with broad maxima at 529 and 562 nm (Figure 6a). Both ferric hemes presumably contribute comparable amounts to the absorption spectrum of AdCytb. Between pH 11 and 12, the spectra undergo a major change with the maximum of the Soret band shifting from 415 to 408 nm and a loss of approximately one-third of the absorbance (Figure 6b). At pH 12, the α and β bands contain only a trace of the peaks observed at lower pH values and a new, broad peak with relatively low intensity appears at 600–620 nm (Figure 6c). These changes are characteristic of a transition from low- to high-spin forms in which both hemes of AdCytb are apparently involved.

Although the transition to a high-spin form is the most conspicuous event, a close examination of the spectra in both the Soret and visual regions suggests the presence of three additional, subtler transitions. Changing the pH from 5.76 to 7.16 leads to a transition that is accompanied by an ~6% absorbance loss in both the Soret and visible regions without any spectral shifts. Between pH 6.9 and 9.2, the peak of the Soret band shifts by 1.5 nm to the red (Figure 6b), while the α and β bands change little. Above pH 9.2 and up to pH 10.9, the Soret peak moves slowly back to shorter wavelengths, while the separation of the α and β maxima decreases by ~5 nm because of the movement of the β maximum to longer wavelengths. Finally, the low-spin AdCytb is transformed to the high-spin species, as described above.

To reconstruct the absorption spectra of the individual pH states of AdCytb and to extract values for the pK of the optical transitions observed by visual inspection of the data, we used nonlinear regression to fit the pH dependence of absorbance changes at each individual wavelength. The number of independent components contributing to the spectra of Adcytb was initially estimated by singular-value decomposition. At first, we considered a model in which AdCytb is a mixture of up to five isoforms, each described by a separate Henderson–Hasselbalch equation with its own pK (see Discussion), but found that the data are better fit with a series of four sequential protonation–deprotonation events of AdCytb according to Scheme 1.

The normalized concentrations of different protonation species in Scheme 1 are as follows:

$$A = 1/Z; \quad (1)$$

$$B = 10^{pH\text{-}pK1}/Z; \quad (2)$$

$$C = 10^{pH\text{-}pK1}10^{pH\text{-}pK2}/Z; \quad (3)$$

$$D = 10^{pH\text{-}pK1}10^{pH\text{-}pK2}10^{pH\text{-}pK3}/Z; \quad (4)$$

$$E = 10^{pH\text{-}pK1}10^{pH\text{-}pK2}10^{pH\text{-}pK3}10^{pH\text{-}pK4}/Z. \quad (5)$$

dx.doi.org/10.1021/bi301127k | *Biochemistry* 2012, 51, 8730–8742

The value of Z can be calculated from the normalization condition: $A + B + C + D + E = 1$, where the values of A–E are given by eqs 1–5.

Figure 7 shows the calculated spectra of the pH-dependent states of AdCytb as defined by Scheme 1. The reconstructed spectra shown over the whole wavelength range (Figure 7a), as well as the details of their line shapes in the Soret (Figure 7b) and visible regions (Figure 7c), are similar to but not identical with the corresponding experimental spectra (Figure 6), reflecting the fact that the former are the spectra of specific pH states of AdCytb while the latter are combinations of these states with overlapping contributions evolving at different pH values. The pK values for each of the individual transitions, calculated for each wavelength, are as follows: pK_1 = 6.5 ± 0.2, pK_2 = 8.3 ± 0.3, pK_3 = 10.5 ± 0.4, and pK_4 = 11.8 ± 0.2 (Figure 7d). To verify the reversibility of optical changes in AdCytb during the pH titration, we repeated the experiment while changing the pH in the opposite direction, starting from pH 9.2 and ending at pH 5.2 (we did not pursue the "reverse" titration at the highest pH values as the high-spin to low-spin transition is a nonphysiological event and is thus not of interest in this context). The pK values yielded by the reverse titration [pK_{1r} = 6.8 ± 0.4, and pK_{2r} = 8.6 ± 0.4 (where r denotes the reverse titration)] were identical within error with the values of pK we obtained in the "direct" titration.

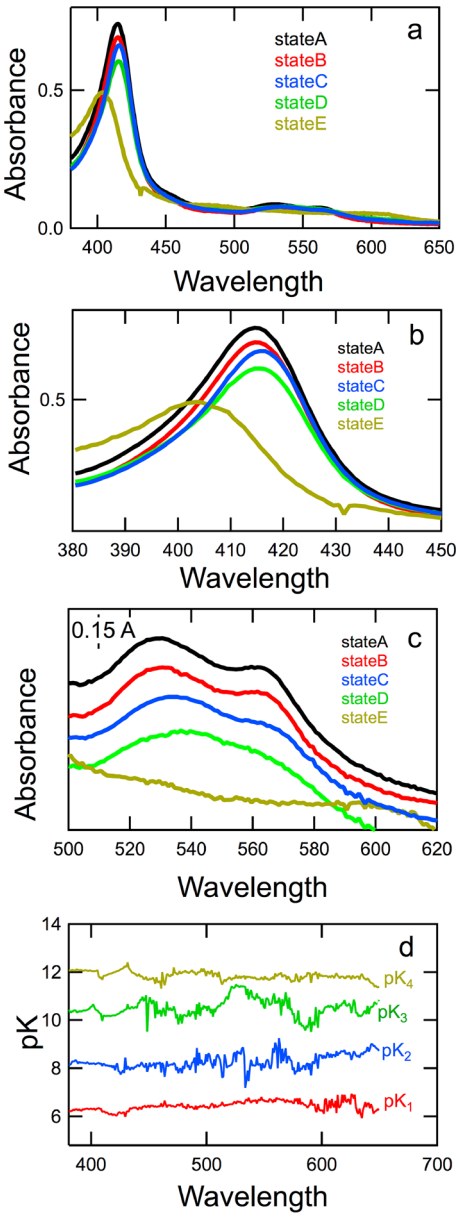

Figure 7. Reconstructed absorption spectra of the different pH states of AdCytb determined according to Scheme 1 and the calculated pK values of the individual transitions between the pH states. (a) Spectra of the pH states of AdCytb reconstructed in the full interval of 380–650 nm. (b) Expanded Soret region. (c) Expanded visible region. The spectra in panel c have been shifted vertically for the sake of clarity. (d) pK values for the individual transitions among states A–E, determined at each wavelength by nonlinear regression of the pH dependence of the absorption spectra of AdCytb according to Scheme 1. Experimental data used for calculation are shown in Figure 6: pK_1 = 6.5 ± 0.2, pK_2 = 8.3 ± 0.3, pK_3 = 10.5 ± 0.4, and pK_4 = 11.9 ± 0.2. Standard deviations were calculated from the pK values obtained at different wavelengths.

The nature of pK_1 is not clear at this stage (see Discussion), but pK_2 can be identified by comparison with the results of EPR and MCD measurements. Thus, pK_2 corresponds to the deprotonation of the high-potential heme; pK_3 characterizes the deprotonation of the low-potential heme, and pK_4 represents the transition from the low-spin to high-spin AdCytb. Although the differences between the spectra of the low-spin pH forms are not large, the reconstructed spectrum of the histidinate form of the high-potential heme is clearly different from the spectrum of the histidinate form of the low-potential heme (compare states C and D in Figure 7c).

Stability of AdCytb at High pH Values. Despite being incubated for up to 6 h at room temperature under potentially adverse conditions of high pH during nIR-MCD and UV–vis experiments, our sample of AdCytb remained completely stable and functional, as judged by the level of its ascorbate reducibility (Figure 8). We prepared solutions of ~9 μM AdCytb in "Buffer A" at pH 6.0, 7.0, 8.0, and 9.0 and used half of each sample for immediate measurements, while the remaining halves were incubated for 24 h before the measurements were repeated. Consecutive spectra of oxidized AdCytb, AdCytb reduced with 30 mM ascorbate, and AdCytb reduced with the addition of a few grains of dithionite were recorded. Figure 8 shows that at pH 9.0 AdCytb is reduced by ascorbate by ~97% both during the initial measurements and after the reduction 24 h later. The spectra of oxidized and reduced AdCytb are practically unaffected by the incubation of oxidized AdCytb and are hardly distinguishable in Figure 8. The absorption of oxidized and reduced AdCytb at pH 9.0 was ~5–7% less than at pH 6.0 (Figure 8, inset), which we interpret as a small difference in the extinction coefficient at two pH values rather than a loss of a heme.

DISCUSSION

Tracing the Histidinate: Evidence from EPR, nIR-MCD, and Absorption Spectra. *EPR Data.* Peisach et al. established parameters for the EPR spectrum of the protoheme–imidazolate compound,[37] thus providing an explanation for the g_z = 2.78–2.84 signal that appears in a number of hemeproteins at high pH. EPR spectra with the same parameters were observed in two types of axial ligation: histidinate–histidine[41,44] and histidinate–methionine.[35] Similar parameters of EPR spectra were observed at high pH for a complex of horse heart metmyoglobin[34] or soybean leghemoglobin[36] with added imidazole (imidazolate; pK ~ 11.0). In our

dx.doi.org/10.1021/bi301127k | Biochemistry 2012, 51, 8730–8742

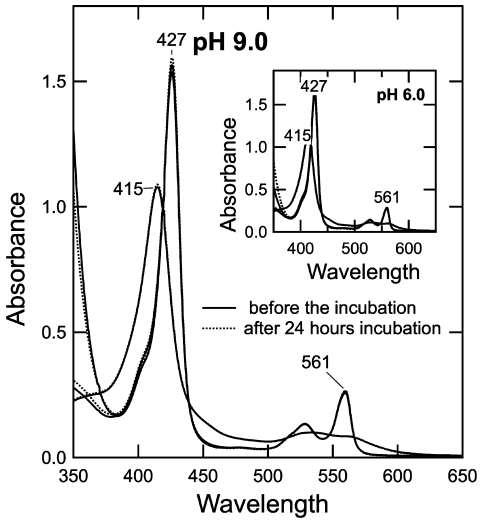

Figure 8. Stability of AdCytb during incubation at pH 9.0 for 24 h. AdCytb (9 μM heme) in "Buffer A" in the presence of 20% glycerol at pH 6.0 (inset), pH 7.0 (not shown), pH 8.0 (not shown), and pH 9.0 (main panel). Oxidized spectra at selected pH values were collected, and the reducibility of AdCytb by 30 mM ascorbate and several grains of dithionite was tested immediately following their consecutive additions (—). A portion of the stock oxidized AdCytb was incubated at room temperature for 24 h, and the reduction by ascorbate and dithionite were repeated (···). The stability of AdCytb at these pH values was such that it is difficult to distinguish the spectra of the 0 and 24 h samples at the three levels of reduction presented here.

experiments, the high-potential heme (g_z = 3.15) of AdCytb undergoes deprotonation of one of its axial ligands (His161 or His88) with a relatively low pK of ~8. The rationalization for the change in the values of pK of Nδ_1 of metal-bound histidine in hemeproteins traditionally includes two components.[51,52] The first is a decrease of 2−3 units from the value of 14 established for free imidazole,[33] resulting from the delocalization of electron density from the heme iron to the imidazole ring.[53] Further lowering of the pK is caused by stabilization of the deprotonated Nδ_1 via hydrogen bonding to an adjacent side group.[35]

The deprotonation of a HALS-type heme that occurs in AdCytb with a pK of ~10.5 is, to the best of our knowledge, reported here for the first time. It is important to note that EPR and MCD signals of a deprotonated HALS heme apparently have the same parameters as a deprotonated conventional low-spin heme; indeed, no new types of signals were observed.

nIR-MCD Data. Gadsby and Thomson were the first to demonstrate the existence of a HisH/His$^-$ pair as a set of axial ligands to the heme by recording the nIR-MCD spectrum of a horse heart metmyoglobin−imidazole complex as a function of pD.[34] They established the parameters of the charge-transfer bands to be 1350/1050 nm; these were later observed for the soybean leghemoglobin−imidazolate complex.[36] Interestingly, unlike EPR, the nIR-MCD spectra of hemeproteins with His$^-$/His and His$^-$/Met coordination exhibit different positions for the corresponding charge-transfer bands. For example, cytochrome b_{562} with its His/Met axial ligands exhibits maxima at 1860/1450 nm at neutral pH that shifts to 1550/1250 nm upon alkalization.[35] The nIR-MCD spectra of AdCytb (Figure 5) show features with maxima at 1650/1350 nm at neutral pD that shift to 1350/1150 nm upon alkalization. Thus, the nIR-MCD spectra of AdCytb, which we believe to be the first collected for any of the proteins of the cytochrome b_{561} family, firmly establish that histidine residues are the only axial ligands to the hemes of AdCytb at any pD between 5.5 and 12.

The characterization of the process of deprotonation of a heme axial ligand histidine with nIR-MCD spectra at room temperature yields a pK that is very close to the value of ~8.0 obtained with EPR, thus confirming that histidinate formation is not a consequence of the liquid helium temperature. nIR-MCD spectra also uniquely help to answer the question of whether the second axial ligand histidine also undergoes deprotonation as the pD becomes increasingly basic. Indeed, Cheesman et al. tabulated the properties of such a species placing its λ_{CT} around 1200 nm,[48] which is overlapping with the low-energy band for the single histidinate−histidine heme complex (Figure 5), precluding our judgment of its existence. On the other hand, there should be a satellite high-energy band for this species, which fails to show up in our experiments (Figure 5). We conclude that there is no evidence of a second axial ligand histidine undergoing deprotonation for either heme in AdCytb within the pD range of our study.

Absorption Data. The pH titration of a protein has the inherent danger of denaturation causing spectral changes that could be mistakenly interpreted as a bona fide spectral feature of that protein. If that were the case for AdCytb, the pH titration in the opposite direction would not yield the same optical transitions as those identified in the direct pH titration. We confirmed the reversibility of the pH titration of AdCytb by showing that the pK values for optical transitions are, within error, identical for titrations in both directions.

The main utility of the mathematical analysis leading to the recovery of the absorption spectra of individual pH forms of AdCytb is the elucidation of the values of pK shown in Scheme 1. Indeed, only the value of pK_2 (the deprotonation of an axial ligand histidine of the high-potential heme) was reliably established by MCD and EPR measurements. A rough estimate of pK_3, characterizing the deprotonation of the axial ligand histidine of the low-potential heme, is provided by EPR, while an approximate value of pK_4 (the formation of the high-spin form of AdCytb) can be deduced from nIR-MCD data. The ability to independently access the pK values of proton acceptor groups of oxidized AdCytb by quantitative analysis of the pH dependence of its absorption spectra is important for this study. On the other hand, the pH-dependent changes in AdCytb absorption spectra were not reported before, and this work associates them with previously established manifestations of histidinate(s) formation in EPR and MCD.[37,48] As the values of pK obtained by three independent methods are remarkably close, this validates the use of absorption spectra in future studies of AdCytb homologues as a simple and less material-consuming test for the state of heme axial ligand(s) protonation compared to the former methods.

The pK values for different species of AdCytb in Scheme 1 are such that there are certain portions of the pH range at which two dissociations are proceeding simultaneously. For instance, at pH 7.5, we observe the dissociation of the last 10% of pK_1 and the first 10% of pK_2. Whether there is cooperativity in this pH range remains to be determined.

Initially, we considered the scenario in which AdCytb is a mixture of up to five isoforms, each described by a pH titration curve consistent with the Henderson−Hasselbalch equation. Although mathematically legitimate, the derived fits were clearly inferior to those obtained using Scheme 1, and

dx.doi.org/10.1021/bi301127k | *Biochemistry* 2012, 51, 8730−8742

furthermore, this would imply AdCytb heterogeneity for which there is no experimental evidence.

The nature of the first transition in Scheme 1 remains an open question. Because it is not accompanied with spectral shifts but can only be followed by the loss of absorption, it can be easily missed. It can result from the conformational change, which leads to a small decrease in the extinction coefficient of AdCytb. Whether the p*K* of ∼6.5 represents a bona fide participant in the mechanism of AdCytb or is merely an artifact of an unrelated pH-dependent process will need to be addressed in the future. One thing can be stated with certainty: the p*K* of 6.5 does not characterize the behavior of the heme axial ligands of AdCytb, as we do not observe this transition by EPR or nIR-MCD, spectral techniques sensitive to the immediate surroundings of hemes, notably its axial ligands. By contrast, the absorption spectra of AdCytb may well be sensitive to groups located beyond the first coordination sphere and thus can provide unique information. Interestingly, there have been several unrelated reports about different activities of AdCytb, which have a pH dependence characterized by a p*K* of ∼6.5, namely, the oxidation of AdCytb with MDA radical and its re-reduction with ascorbate observed in pulse radiolysis experiments,[54] and of interaction of membranous AdCytb with ascorbate and its inhibition with DEPC modification.[8,31]

Temperature-Dependent pH Changes of Buffers. To be able to compare the results of EPR experiments performed at 8 K with the results of nIR-MCD and absorption spectroscopy conducted at room temperature, one has to be confident that the pH values measured at room temperature in all three experiments can be compared. Meanwhile, temperature-dependent pH changes are a well-known phenomenon that must be considered.[47] The buffer composition is the most important factor controlling temperature-dependent pH changes. We have chosen to use Good buffers[40] following Orii and Morita,[45] who observed that shifts in pH caused by freezing are less than 1 pH unit in their presence, while phosphate and TRIS, the buffers most often used in the AdCytb field, can cause 2−3 unit shifts toward acidic and basic pH values, respectively, depending on concentration.[46,47] The data for HEPES, which is also often used in AdCytb studies, are contradictory. It was used to compensate for the acidic changes introduced by phosphate in an attempt to develop a temperature-independent buffer,[46] but Williams-Smith et al.[47] reported that HEPES shifts the pH on freezing in the same direction as phosphate. The presence of protein and glycerol in the buffer moderates the pH shifts.[45−47] In addition, glycerol is reported to be a glassing agent causing fewer artifacts in EPR spectra than sucrose and ethylene glycol.[55] Finally, the manner in which the freezing of the sample is performed also affects the outcome.[47] Given the multiplicity of factors affecting shifts in pH occurring on freezing, it is not surprising that the observations of the g_z = 2.84 EPR signal of His^--AdCytb in EPR[18,19,56] have been inconsistent. In this study, we did not try to prevent a pH shift on freezing of the samples but focused on minimizing and calibrating it while monitoring the results. As observed in pilot experiments, cooling "Buffer A" in the presence of glycerol and a universal pH indicator shifted the pH to more basic values but by no more than 0.25−0.5 unit between pH 7.0 and 10 (the useful range of the indicator employed). At pH values between 5.5 and 7.0, there were no detectable shifts in pH. We assume that the pH of our samples did not change significantly upon further cooling to 8 K, as was shown by Sieraki et al.[46] A correction of 0.5 unit to the p*K* of His^--AdCytb deduced from the EPR measurements was in good agreement with the p*K* obtained at room temperature, by both MCD and UV−vis.

Bona Fide pH-Dependent Changes versus pH-Dependent Denaturation. There are reports that purified samples of AdCytb exhibit peculiarly slow kinetic behavior at pH <6.0[57] and show significant denaturation upon mild alkalization.[38,56] In the experiments of Wanduragala et al., incubation of oxidized AdCytb at pH 8.0 for just 1 h led to a shift of the Soret band from the usual value of 415 to 410 nm that can be associated with the appearance of a high-spin heme EPR spectrum.[56] Similar phenomena were observed by Okuyama et al. after overnight incubation of oxidized AdCytb at pH 8.4.[38] In both studies, the reducibility of AdCytb with ascorbate was significantly decreased, presumably as a consequence of a lowering of the redox potential of AdCytb and/or partial disruption of the ascorbate binding centers.

It is important not to confuse the changes caused by pH-dependent protein denaturation[38,56] for genuine transitions between different pH forms of AdCytb. In our experiments with oxidized AdCytb, the high-spin species appeared with p*K* values of 11.6 (nIR-MCD) or 11.7 (UV−vis); the first increase in the magnitude of the high-spin signal above background occurring in EPR is also above pH 11.

We have previously reported that the ascorbate reducibility of AdCytb is stable for 2 h in the pH range of 5−10.[39] In the experiments reported here, we incubated AdCytb at gradually increasing pH values for up to 6 h. To compare our preparation of AdCytb with that of both Okuyama et al.[38] and Wandarugala et al.,[56] we incubated oxidized AdCytb at room temperature for 24 h at pH 6.0, 7.0, 8.0, and 9.0 (Figure 8), and subsequent inspection did not find any changes in absorption spectra or in reducibility with ascorbate.

One obvious difference between this study and those of Okuyama et al.[38] and Wandarugala et al.[56] is the identity of the detergents used. We have conducted all of our experiments using dodecyl *β*-maltoside, while previous workers employed *β*-octyl glucoside.[38,56] It may be important that our data on the behavior of AdCytb in analytical ultracentrifugation (da Silva, Kamensky, Musatov, and Palmer, unpublished observations) show that AdCytb exhibits a much higher level of heterogeneity in *β*-octyl glucoside than in dodecyl *β*-maltoside. A recently published report on two plant cytochromes b_{561} expressed in *E. coli* and purified with dodecyl *β*-maltoside documents a much more stable protein over a broad pH range.[27] We thus conclude that the changes in protonation of AdCytb reported here are intrinsic properties of the cytochrome and are not the result of a pH-dependent denaturation.

Updated Concerted Electron−Proton-Transfer Mechanism for AdCytb. Njus, Kelley, and colleagues[5,8] introduced the first general mechanism for the oxidation of ascorbic acid by AdCytb in the framework of the concept of concerted proton−electron transfer from organic substrates. The central element of the mechanism is the binding of ascorbate monoanion to the N*ε* atom of a histidine residue (Figure 9A) located in a putative ascorbate-binding center on the cytoplasmic interface of AdCytb. Binding to AdCytb destabilizes the ascorbate monoanion and stabilizes monodehydroascorbate radical, $MDA^{\bullet-}$, the product of its oxidation.[8] This process affects the redox potential of this pair, making possible the effective reduction of AdCytb.[c]

The salient feature of this mechanism is that all the chemistry of ascorbate oxidation is controlled by the apoprotein and the

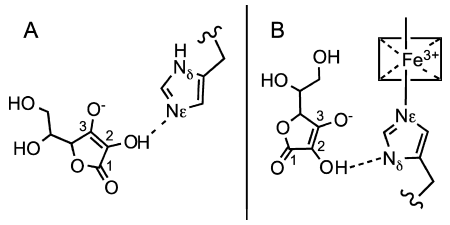

Figure 9. Interaction of AdCytb with ascorbate via the histidine residue. A comparison of the key elements of the mechanisms introduced by Njus et al.[8] (A) and further modified by Nakanishi et al.[24] (B). The details are given in the text.

heme merely serves as a sink for electrons abstracted from ascorbate.[8] To the extent that model systems are capable of reproducing the processes that occur in proteins, the benefit of involving a redox cofactor in the process of ascorbate oxidation is illustrated by comparison of the results of the studies by Kipp et al.[9] and Warren and Mayer.[32] While the facilitation of ascorbate oxidation in solution by free imidazole had a second-order constant[d] of 17 M^{-1} s^{-1},[9] a staggering rate of 10^6–10^8 M^{-1} s^{-1} was reported for ascorbate oxidation by an iron–porphyrin–imidazole complex.[32] Recently, Tsubaki and his colleagues[24] developed further the mechanism of ascorbate oxidation by suggesting that the deprotonated histidine axial ligand of AdCytb binds the ascorbate via Nδ of the imidazole heterocycle (Figure 9B), thus engaging the heme's redox properties in the process.

The data presented here support the involvement of a histidinate axial ligand in the oxidation of ascorbate by AdCytb. Figure 10 presents the AdCytb mechanism, in which features of the original scheme of Njus et al.,[5,8] modified by Nakanishi et al.,[24] are combined with three new refinements that we are proposing.

First, we locate the high-potential heme on the cytoplasmic interface of AdCytb in place of the low-potential heme invoked in the model of Nakanishi et al.[24] Indeed, if the deprotonated axial ligand is a mandatory participant in the AdCytb mechanism, it should be located on the cytoplasmic interface of the cytochrome where the oxidation of ascorbate takes place. The heme with a pK relevant to physiological conditions of chromaffin cells (the pH in the cytoplasm is 7.2[21]) is the high-potential heme (g_z = 3.15); thus, it must be located on the cytoplasmic interface of AdCytb if concerted H^+/e^- transfer is operational. This conclusion is fully consistent with the predictions from the experiments of Desmet et al.[29] with plant cytochrome b_{561} and of our group with AdCytb.[19,25,26]

Second, we introduce the help of a general base for abstracting the proton from the axial ligand histidine of oxidized AdCytb. Putative candidates for that role are glutamine 79, arginine 82, and lysine 85, residues located in the third extramembrane segment.[26] It was noted previously that Nδ_1 of the histidine ligand is H-bonded in the majority of known crystal structures of cytochromes.[51,52,58] Third, our model does not include a device for controlling the release of a proton and $MDA^{\bullet-}$ from AdCytb upon interaction with a new molecule of ascorbate, as initially suggested by Nakanishi et al.[24] In our version of the model, the protonation or deprotonation of Nδ_1 of the axial ligand histidine depends directly on the redox status of the high-potential heme.

In conclusion, we note that the ability of one of the axial histidines to the high-potential heme of AdCytb to undergo deprotonation with a pK of ∼8.0 is firmly established by the

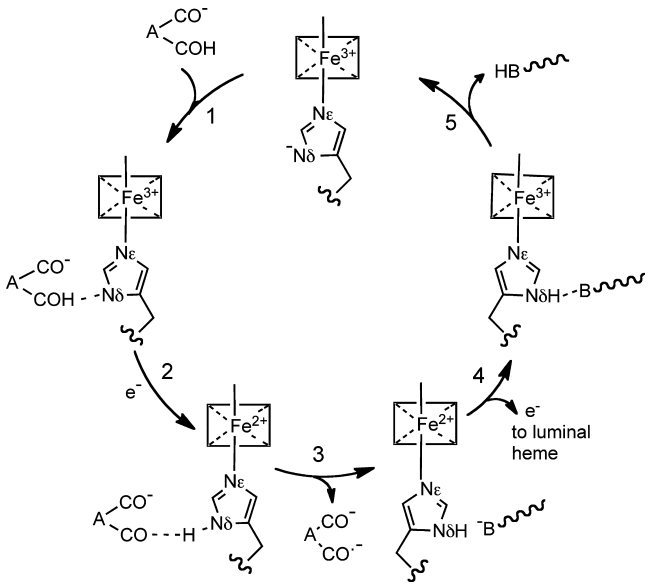

Figure 10. Updated mechanism of AdCytb. The scheme is based on the mechanism originally proposed by Njus et al.,[8] modified by Nakanishi et al.,[24] with our additional amendments. In the resting state, the oxidized high-potential heme of AdCytb has one histidine ligand partially deprotonated (Nδ^-); a pK of ∼8.0 was established for the purified protein (Figures 3–7) but may be lower in the chromaffin granule membrane environment. Ascorbate has one hydroxyl group (C-3) deprotonated and binds to Nδ^- via its hydroxyl on C-2. (2) Binding to AdCytb makes the ascorbate–MDA monoanion pair a stronger reductant, permitting it to reduce the high-potential heme and forming the protonated monodehydroascorbate radical. Upon reduction, the pK of Nδ^- shifts to a higher value because of the redox Bohr effect,[59] and the proton from C-2 of ascorbate binds to Nδ^-. NδH and $MDA^{\bullet-}$ are formed in a process of concerted H^+/e^- transfer. (3) The monodehydroascorbate anion dissociates from the complex of ascorbate with AdCytb. (4) The electron present on the high-potential heme is transferred to the low-potential heme. The value of the pK of Nδ is restored to 8.0, which is characteristic of oxidized AdCytb. (5) The oxidized high-potential heme transfers the proton to a neighboring amino acid (B^-), which functions as a general base. The deprotonated oxidized high-potential heme then is available for a new reaction cycle.

good agreement of data derived from the three independent spectroscopic methods we employed. The low-potential heme of AdCytb has a pK of ∼10.5, making it an unlikely candidate for accepting a proton in the physiological pH range. Thus, the current mechanism of AdCytb reduction is predicated on the interaction of cytoplasmic ascorbate with the axial ligand histidinate of the high-potential heme. The involvement of an additional proton acceptor group (pK ∼ 6.5) in the mechanism of AdCytb is a possibility that needs to be further investigated.

AUTHOR INFORMATION

Corresponding Author

*Y.A.K.: telephone, (713) 348-3903; fax, (713) 348-5154; e-mail, yuryk@rice.edu. G.P.: telephone, (713) 348-4860; fax, (713) 348-5154; e-mail, graham@rice.edu.

Funding

This work was supported by National Institutes of Health (NIH) Grant GM 080575 to G.P. and by an NIH National Research Service Award Individual Fellowship to G.F.Z.d.S. #FGM086059A.

Notes

The authors declare no competing financial interest.

■ ACKNOWLEDGMENTS

We are indebted to Dr. Ah-Lim Tsai (University of Texas Health Science Center at Houston) for his assistance with EPR and MCD experiments and many helpful discussions. We are grateful to Dr. F. Ann Walker (University of Arizona, Tucson, AZ) for helpful advice on executing our experimental plan. We thank Dr. Myles Cheesman and Dr. Andrew Thomson (University of East Anglia, Norwich, U.K.) for the discussion of our nIR-MCD results and Drs. Michael Johnson and Evert Duin (The University of Georgia, Athens, GA) for collecting liquid helium spectra of membranous AdCytb at earlier stages of this work.

■ ABBREVIATIONS

AdCytb, adrenal cytochrome b_{561}; HisH-AdCytb, cytochrome b_{561} with protonated axial ligand histidine; His^-- AdCytb, cytochrome b_{561} with histidinate as an axial ligand; $HisH^+$, histidine amino residue (nonligand) protonated at the Nε atom; MDA, monodehydroascorbate; $MDA^{\bullet}$, monodehydroascorbate radical; $MDA^{\bullet-}$, monodehydroascorbate radical anion; EPR, electron paramagnetic resonance; HALS, highly axial low-spin signal; E_m, midpoint redox potential at pH 7.0; nIR-MCD, near-infrared magnetic circular dichroism; DEPC, diethyl pyrocarbonate; EDTA, ethylenediaminetetraacetic acid; DM, *n*-dodecyl β-D-maltoside; MES, 2-(*N*-morpholino)-ethanesulfonic acid; MOPS, 3-(*N*-morpholino)propanesulfonic acid; TRIS, 2-amino-2-(hydroxymethyl)propane-1,3-diol; TAPS, *N*-tris(hydroxymethyl)methyl-3-aminopropanesulfonic acid; CAPS, *N*-cyclohexyl-3-aminopropanesulfonic acid; IPTG, isopropyl β-D-galactopyranoside.

■ ADDITIONAL NOTES

[a]HALS stands for highly anisotropic low-spin heme[1] or for highly axial low-spin heme.[2] It is also in the literature called the g_{max} EPR signal (g_{max} > 3.3) and is a type I heme according to the nomenclature introduced by Walker.[3]

[b]Among hundreds of known hemeproteins, only two cases of the involvement of Nδ_1 in heme ligation are known: cytochrome c_{554} and a Met65His mutant of cellobiose dehydrogenase.[4]

[c]In solution, the midpoint redox potential of the monoanion ascorbate/$MDA^{\bullet-}$ pair is 766 mV,[5] which makes it a poor reductant for the high-potential heme of AdCytb with its E_m of 170 mV.[6,7] Molecular modeling calculations of hydrogen bond energy showed that bonding of the unprotonated Nε atom of imidazole to the 2-hydroxyl of ascorbate monoanion would make the bond energy stronger for the radical versus monoanion ascorbate.[8]

[d]The second-order rate constant was calculated by dividing the first-order constant of 5 s^{-1} by the equilibrium concentration of 0.3 M, both reported in Table 1 of Kipp et al.[9]

■ REFERENCES

(1) Migita, C., and Iwaizumi, M. (1981) Low-temperature EPR studies of highly anisotropic low-spin (protoporphyrinato)iron(III) complexes. *J. Am. Chem. Soc. 103*, 4378−4381.

(2) Salerno, J. C. (1984) Cytochrome electron spin resonance line shapes, ligand fields, and components stoichiometry in ubiquinol-cytochrome c oxidoreductase. *J. Biol. Chem. 259*, 2331−2336.

(3) Walker, F. (1999) Magnetic spectroscopy (EPR, ESEEM, Mösbauer, MCD, and NMR) studies of low-spin ferriheme centers and their corresponding heme proteins. *Coord. Chem. Rev. 185−186*, 471−534.

(4) Turano, P., and Lu, Y. (2001) Iron in heme and related proteins. In *Handbook on Metalloproteins* (Bertini, I., Sigel, A., and Sigel, H., Eds.) pp 269−356, Marcel Dekker, Inc., New York.

(5) Njus, D., and Kelley, P. M. (1993) The secretory-vesicle ascorbate-regenerating system: A chain of concerted H^+/e^--transfer reactions. *Biochim. Biophys. Acta 1144*, 235−248.

(6) Apps, D. K., Boisclair, M. D., Gavine, F. S., and Pettigrew, G. W. (1984) Unusual redox behaviour of cytochrome b-561 from bovine chromaffin granule membranes. *Biochim. Biophys. Acta 764*, 8−16.

(7) Takeuchi, F., Kobayashi, K., Tagawa, S., and Tsubaki, M. (2001) Ascorbate inhibits the carbethoxylation of two histidyl and one tyrosyl residues indispensable for the transmembrane electron transfer reaction of cytochrome b_{561}. *Biochemistry 40*, 4067−4076.

(8) Njus, D., Wigle, M., Kelley, P., Kipp, B. H., and Schlegel, B. H. (2001) Mechanism of ascorbic acid oxidation by cytochrome b561. *Biochemistry 40*, 11904−11911.

(9) Kipp, B. H., Faraj, C., Li, G., and Njus, D. (2004) Imidazole facilitates electron transfer from organic reductants. *Bioelectrochemistry 64*, 7−13.

(10) Verelst, W., and Asard, H. (2003) A phylogenetic study of cytochrome b_{561} proteins. *Genome Biol. 4*, R38.

(11) Tsubaki, M., Takeuchi, F., and Nakanishi, N. (2005) Cytochrome b_{561} protein family: Expanding roles and versatile transmembrane electron transfer abilities as predicted by a new classification system and protein sequence motif analyses. *Biochim. Biophys. Acta 1753*, 174−190.

(12) Apps, D. K. (1997) Membrane and soluble proteins of adrenal chromaffin granules. *Semin. Cell Dev. Biol. 8*, 121−131.

(13) Ohtani, S., Iwamaru, A., Deng, W., Ueda, K., Wu, G., Jayachandran, G., Kondo, S., Atkinson, E. N., Minna, J. D., Roth, J. A., and Ji, L. (2007) Tumor suppressor 101F6 and ascorbate synergistically and selectively inhibit non-small cell lung cancer growth by caspase-independent apoptosis and autophagy. *Cancer Res. 67*, 6293−6303.

(14) Su, D., May, J. M., Koury, M. J., and Asard, H. (2006) Human erythrocyte membranes contain a cytochrome b_{561} that may be involved in extracellular ascorbate recycling. *J. Biol. Chem. 281*, 39852−39859.

(15) McKie, A. T., Barrow, D., Latunde-Dada, G. O., Rolfs, A., Sager, G., Mudaly, E., Mudaly, M., Richardson, C., Barlow, D., Bomford, A., Peters, T. J., Raja, K. B., Shirali, S., Hediger, M. A., Farzaneh, F., and Simpson, R. J. (2001) An iron-regulated ferric reductase associated with the absorption of dietary iron. *Science 291*, 1755−1759.

(16) Burbaev, D., Moroz, I. A., Kamenskiy, Y. A., and Konstantinov, Au. A. (1991) Several forms of chromaffin granule cytochrome b-561 revealed by EPR spectroscopy. *FEBS Lett. 283*, 97−99.

(17) Kamensky, Y. A., and Palmer, G. (2001) Chromaffin granule membranes contain at least three heme centers: Direct evidence from EPR and absorption spectroscopy. *FEBS Lett. 491*, 119−122.

(18) Tsubaki, M., Nakayama, M., Okuyama, E., Ichikawa, Y., and Hori, H. (1997) Existence of two heme B centers in cytochrome b_{561} from bovine adrenal chromaffin vesicles as revealed by a new purification procedure and EPR spectroscopy. *J. Biol. Chem. 272*, 23206−23210.

(19) Kamensky, Y., Liu, W., Tsai, A. L., Kulmacz, R. J., and Palmer, G. (2007) Axial ligation and stoichiometry of heme centers in adrenal cytochrome b_{561}. *Biochemistry 46*, 8647−8658.

(20) Njus, D., Zallakian, M., and Knoth, J. (1981) The chromaffin granule: Proton-cycling in the slow lane. In *Chemiosmotic Proton Circuits in Biological Membranes* (Skulachev, V. P., and Hinkle, P. C., Eds.) pp 365−374, Addison-Wesley Publishing Co., Inc., Reading, MA.

(21) Kao, L. S., Ho, M. Y., and Cragoe, E. J., Jr. (1991) Intracellular pH and catecholamine secretion from bovine adrenal chromaffin cells. *J. Neurochem. 57*, 1656−1660.

(22) Tsubaki, M., Kobayashi, K., Ichise, T., Takeuchi, F., and Tagawa, S. (2000) Diethyl pyrocarbonate modification abolishes fast electron accepting ability of cytochrome b_{561} from ascorbate but does not influence electron donation to monodehydroascorbate radical: Identification of the modification sites by mass spectrometric analysis. *Biochemistry 39*, 3276−3284.
(23) Takeuchi, F., Hori, H., Obayashi, E., Shiro, Y., and Tsubaki, M. (2004) Properties of two distinct heme centers of cytochrome b_{561} from bovine chromaffin vesicles studied by EPR, resonance Raman, and ascorbate reduction assay. *J. Biochem. 135*, 53−64.
(24) Nakanishi, N., Takeuchi, F., and Tsubaki, M. (2007) Histidine cycle mechanism for the concerted proton/electron transfer from ascorbate to the cytosolic haem b centre of cytochrome b_{561}: A unique machinery for the biological transmembrane electron transfer. *J. Biochem. 142*, 553−560.
(25) Liu, W., Rogge, C. E., da Silva, G. F., Shinkarev, V. P., Tsai, A. L., Kamensky, Y., Palmer, G., and Kulmacz, R. J. (2008) His92 and His110 selectively affect different heme centers of adrenal cytochrome b_{561}. *Biochim. Biophys. Acta 1777*, 1218−1228.
(26) Liu, W., da Silva, G. F., Wu, G., Palmer, G., Tsai, A. L., and Kulmacz, R. J. (2011) Functional and structural roles of residues in the third extramembrane segment of adrenal cytochrome b_{561}. *Biochemistry 50*, 3149−3160.
(27) Cenacchi, L., Busch, M., Schleidt, P. G., Muller, F. G., Stumpp, T. V., Mantele, W., Trost, P., and Lancaster, C. R. (2012) Heterologous production and characterisation of two distinct dihaem-containing membrane integral cytochrome b_{561} enzymes from *Arabidopsis thaliana* in *Pichia pastoris* and *Escherichia coli* cells. *Biochim. Biophys. Acta 1818*, 679−688.
(28) Nakanishi, N., Rahman, M. M., Sakamoto, Y., Miura, M., Takeuchi, F., Park, S. Y., and Tsubaki, M. (2009) Inhibition of electron acceptance from ascorbate by the specific N-carbethoxylations of maize cytochrome b_{561}: A common mechanism for the transmembrane electron transfer in cytochrome b_{561} protein family. *J. Biochem. 146*, 857−866.
(29) Desmet, F., Berczi, A., Zimanyi, L., Asard, H., and Van Doorslaer, S. (2011) Axial ligation of the high-potential heme center in an *Arabidopsis* cytochrome b_{561}. *FEBS Lett. 585*, 545−548.
(30) Jalukar, V., Kelley, P. M., and Njus, D. (1991) Reaction of ascorbic acid with cytochrome b_{561}. Concerted electron and proton transfer. *J. Biol. Chem. 266*, 6878−6882.
(31) Kipp, B. H., Kelley, P. M., and Njus, D. (2001) Evidence for an essential histidine residue in the ascorbate-binding site of cytochrome b_{561}. *Biochemistry 40*, 3931−3937.
(32) Warren, J. J., and Mayer, J. M. (2008) Hydrogen atom transfer reactions of iron-porphyrin-imidazole complexes as models for histidine-ligated heme reactivity. *J. Am. Chem. Soc. 130*, 2774−2776.
(33) George, G. I. H., Hanania, G., Irvine, D. H., and Abu-Issa, I. (1964) The effect of co-ordination on ionization. Part IV. Imidazole and its ferrimyoglobin complex. *J. Chem. Soc.*, 5689−5694.
(34) Gadsby, P. M., and Thomson, A. J. (1982) Identification of the imidazolate anion as a ligand in met-myoglobin by near-infrared magnetic circular dichroism spectroscopy. *FEBS Lett. 150*, 59−63.
(35) Moore, G. R., Williams, R. J., Peterson, J., Thomson, A. J., and Mathews, F. S. (1985) A spectroscopic investigation of the structure and redox properties of *Escherichia coli* cytochrome b-562. *Biochim. Biophys. Acta 829*, 83−96.
(36) Sievers, G., Gadsby, P. M., Peterson, J., and Thomson, A. J. (1983) Magnetic circular dichroism spectra of soybean leghaemoglobin a at room temperature and 4.2 K. *Biochim. Biophys. Acta 742*, 637−647.
(37) Peisach, J., Blumberg, W. E., and Adler, A. (1973) Electron paramagnetic resonance studies of iron porphin and chlorin systems. *Ann. N.Y. Acad. Sci. 206*, 310−327.
(38) Okuyama, E., Yamamoto, R., Ichikawa, Y., and Tsubaki, M. (1998) Structural basis for the electron transfer across the chromaffin vesicle membranes catalyzed by cytochrome b_{561}: Analyses of cDNA nucleotide sequences and visible absorption spectra. *Biochim. Biophys. Acta 1383*, 269−278.
(39) Liu, W., Rogge, C. E., Kamensky, Y., Tsai, A. L., and Kulmacz, R. J. (2007) Development of a bacterial system for high yield expression of fully functional adrenal cytochrome b_{561}. *Protein Expression Purif. 56*, 145−152.
(40) Good, N. E., Winget, G. D., Winter, W., Connolly, T. N., Izawa, S., and Singh, R. M. (1966) Hydrogen ion buffers for biological research. *Biochemistry 5*, 467−477.
(41) Bois-Poltoratsky, R., and Ehrenberg, A. (1967) Magnetic and spectrophotometric investigations of cytochrome b_5. *Eur. J. Biochem. 2*, 361−365.
(42) Brautigan, D. L., Feinberg, B. A., Hoffman, B. M., Margoliash, E., Preisach, J., and Blumberg, W. E. (1977) Multiple low spin forms of the cytochrome c ferrihemochrome. EPR spectra of various eukaryotic and prokaryotic cytochromes c. *J. Biol. Chem. 252*, 574−582.
(43) Watari, H., Groudinsky, O., and Labeyrie, F. (1967) Electron spin resonance of cytochrome b_2 and of b_2 core. *Biochim. Biophys. Acta 131*, 592−594.
(44) Ikeda, M., Iizuka, T., Takao, H., and Hahihara, B. (1974) Studies on the heme environment of oxidized cytochrome b_5. *Biochim. Biophys. Acta 336*, 15−24.
(45) Orii, Y., and Morita, M. (1977) Measurement of the pH of frozen buffer solutions by using pH indicators. *J. Biochem. 81*, 163−168.
(46) Sieracki, N. A., Hwang, H. J., Lee, M. K., Garner, D. K., and Lu, Y. (2008) A temperature independent pH (TIP) buffer for biomedical biophysical applications at low temperatures. *Chem. Commun.*, 823−825.
(47) Williams-Smith, D. L., Bray, R. C., Barber, M. J., Tsopanakis, A. D., and Vincent, S. P. (1977) Changes in apparent pH on freezing aqueous buffer solutions and their relevance to biochemical electron-paramagnetic-resonance spectroscopy. *Biochem. J. 167*, 593−600.
(48) Cheesman, M. R., Greenwood, C., and Thomson, A. J. (1991) Magnetic circular dichroism of hemoproteins. *Adv. Inorg. Chem. 36*, 201−250.
(49) Finnegan, M. G., Knaff, D. B., Qin, H., Gray, K. A., Daldal, F., Yu, L., Yu, C.-A., Kleis-San Francisco, S., and Johnson, M. K. (1996) Axial heme ligation in the cytochrome bc_1 complexes of mitochondrial and photosynthetic membranes. A near-infrared magnetic circular dichroism and electron paramagnetic resonance study. *Biochim. Biophys. Acta 1274*, 9−20.
(50) Sievers, G., Gadsby, P. M., Peterson, J., and Thomson, A. J. (1983) Assignment of the axial ligands of the haem in milk lactoperoxidase using magnetic circular dichroism spectroscopy. *Biochim. Biophys. Acta 742*, 659−668.
(51) Weber, P. C. (1982) Correlations between structural and spectroscopic properties of the high-spin heme protein cytochrome c′. *Biochemistry 21*, 5116−5119.
(52) Bowman, S. E., and Bren, K. L. (2010) Variation and analysis of second-sphere interactions and axial histidinate character in c-type cytochromes. *Inorg. Chem. 49*, 7890−7897.
(53) Gadsby, P., and Thomson, A. (1986) Low-temperature EPR and near-infrared MCD studies of highly anisotropic low-spin ferrihaem complexes. *FEBS Lett. 197*, 253−257.
(54) Kobayashi, K., Tsubaki, M., and Tagawa, S. (1998) Distinct roles of two heme centers for transmembrane electron transfer in cytochrome b561 from bovine adrenal chromaffin vesicles as revealed by pulse radiolysis. *J. Biol. Chem. 273*, 16038−16042.
(55) Gadsby, P. M., Peterson, J., Foote, N., Greenwood, C., and Thomson, A. J. (1987) Identification of the ligand-exchange process in the alkaline transition of horse heart cytochrome c. *Biochem. J. 246*, 43−54.
(56) Wanduragala, S., Wimalasena, D. S., Haines, D. C., Kahol, P. K., and Wimalasena, K. (2003) pH-induced alteration and oxidative destruction of heme in purified chromaffin granule cytochrome b_{561}: Implications for the oxidative stress in catecholaminergic neurons. *Biochemistry 42*, 3617−3626.
(57) Takigami, T., Takeuchi, F., Nakagawa, M., Hase, T., and Tsubaki, M. (2003) Stopped-flow analyses on the reaction of ascorbate

with cytochrome b_s purified from bovine chromaffin vesicle membranes. *Biochemistry 42*, 8110−8118.
(58) Landrum, J. T., Hatano, K., Scheidt, W. R., and Reed, C. A. (1980) Imidazolate complexes of iron and manganese. *J. Am. Chem. Soc. 102*, 6729−6735.
(59) Chance, B. (1972) The nature of electron transfer and energy coupling reactions. *FEBS Lett. 23*, 3−20.